ORGANOMETALLICS

ARTICLE

pubs.acs.org/Organometallics

Hydroboration of Disilyne RSi≡SiR (R = Si^{i}Pr[CH(SiMe$_3$)$_2$]$_2$), Giving Boryl-Substituted Disilenes

Katsuhiko Takeuchi, Masaaki Ichinohe, and Akira Sekiguchi*

Department of Chemistry, Graduate School of Pure and Applied Sciences, University of Tsukuba, Tsukuba, Ibaraki 305-8571, Japan

Supporting Information

ABSTRACT: The reaction of 1,1,4,4-tetrakis[bis(trimethylsilyl)methyl]-1,4-diisopropyltetrasila-2-yne (**1**) with hydroboranes afforded boryl-substituted disilenes R(R′$_2$B)Si═SiHR **3a** and **3b** (R = Si^{i}Pr[CH(SiMe$_3$)$_2$]$_2$, R′$_2$B = 9-borabicyclo[3.3.1]nonan-9-yl (**3a**), catecholboryl (**3b**)). Spectroscopic and X-ray crystallographic analyses of **3a** and **3b** showed that **3a** has a nearly coplanar arrangement of the Si═Si double bond and the boryl group, allowing π-conjugation between them, whereas **3b**, with a markedly twisted arrangement, exhibits no such conjugation. Theoretical calculations suggest that π-conjugation between the π-orbital of the Si═Si double bond and the vacant 2p-orbital on the boron atom is markedly influenced by the dihedral angle between the Si═Si double-bond plane and boryl group plane.

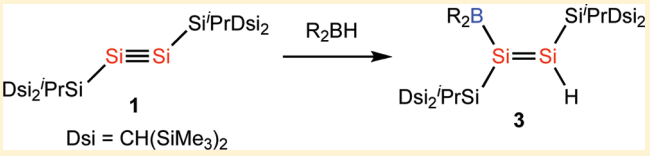

INTRODUCTION

The chemistry of multiply bonded compounds containing heavier group 14 elements has been developed since the isolation of the stable distannene Dsi$_2$Sn═SnDsi$_2$ (Dsi = CH(SiMe$_3$)$_2$) by Lappert in 1973[1] and tetramesityldisilene Mes$_2$Si═SiMes$_2$ (Mes = 2,4,6-trimethylphenyl)[2] and the silene (Me$_3$Si)$_2$Si═C(OSiMe$_3$)Ad (Ad = 1-adamantyl) in 1981.[3,4] In addition to alkene analogues of heavier group 14 elements, the synthesis and structural characterization of the heavier alkyne analogues have been described in the literature:[5] lead and tin analogues were reported by Power's group,[6,7] germanium analogues were reported by Power's group[8] and Tokitoh's group,[9] and silicon analogues, disilynes, have been synthesized by our group,[10] Wiberg's group,[11] and Tokitoh's group[12] using very bulky silyl groups or aryl groups for kinetic stabilization. Unsymmetically substituted disilyne was also recently reported.[13]

The first isolable crystalline disilyne, **1**, RSi≡SiR (R = Si^{i}Pr[CH(SiMe$_3$)$_2$]$_2$), has two nondegenerate highest occupied π-MOs and lowest unoccupied π^*-MOs with a slight contribution from the antibonding σ^*(Si−Si)-orbital of the central bond because of its *trans*-bent structure.[10] Therefore, disilyne **1** has a relatively small HOMO−LUMO gap, which accounts for its higher reactivity toward alkenes,[14] alkynes,[14] alkyllithium,[15,16] alkali metals,[15,17] nitriles,[18] and silylcyanides[19,20] to afford 1,2-disilacyclobutenes, 1,2-disilabenzene derivatives, disilenyllithiums, anion radicals, triaza-1,4-disilabicyclo[2.2.2]oct-2,5,7-triene derivatives, disilyne−silylisocyanide bis-adduct, and 1,4-diaza-2,3-disilabenzene derivatives, respectively. Wiberg's group and Tokitoh's group also reported the reaction of disilynes with alkenes,[11,21] dienes,[11,21] and alkynes.[22] Very recently, we also reported the reaction of **1** with NHC (N-heterocyclic carbene), giving an NHC−disilyne complex R(L)Si═SiR: (L = NHC).[23] However, several studies of disilynes indicate that all reactions of disilynes with small organic molecules involve an interaction between the LUMO (π_{in}^*) of the disilyne and the HOMO of the organic molecules.[14−23]

Recently, we reported the synthesis of two amino-substituted disilenes R(R′$_2$N)Si═SiHR (R′$_2$N = Et$_2$N (**2a**) or Ph$_2$N (**2d**)) by the reaction of disilyne **1** with diethylamine or diphenylamine.[24] The NMR spectral data of **2a** and **2b** show that **2a** has π-conjugation between the Si═Si double bond and the lone pair on the nitrogen atom with a coplanar arrangement of the Si═Si double bond and the amino group, whereas **2b** exhibits little such conjugation because of the nearly perpendicular Si═Si double bond and the amino group plane. We also reported the synthesis of boryl-substituted disilene R(R′$_2$B)Si═SiHR **3a** (R′$_2$B = 9-bora[3.3.1]nonan-9-yl) by reaction of **1** with 9-borabicyclo[3.3.1]nonane (9-BBN), which has π-conjugation between the Si═Si double bond and the vacant 2p-orbital on the boron atom because of the coplanar arrangement of its Si═Si double bond and the boryl group.[24a] We also reported the boryl-substituted disilenes (^{t}Bu$_2$MeSi)$_2$Si═Si(SiMe^{t}Bu$_2$)(BR*$_2$) **4a**,**b** (R* = pinacol (**4a**), catechol (**4b**)),[25] which have little π-conjugation because of the almost perpendicular orientation of the boryl substituent to the Si═Si double bond plane, prepared by the reaction of disilenyllithium (^{t}Bu$_2$MeSi)$_2$Si═Si(SiMe^{t}Bu$_2$)Li with *B*-chloropinacolborane, (pin)BCl, or *B*-chlorocatecholborane, (cat)BCl, respectively. However, the properties of **3a** and **4a**,**b** cannot be compared with each other because their substituents are completely different. In this report, we present details of the synthesis and properties of boryl-substituted disilenes R(R′$_2$B)Si═SiHR (R′$_2$B = 9-bora[3.3.1]nonan-9-yl (**3a**) and catecholboryl (**3b**)) by the reactions of disilyne **1** with hydroboranes, 9-BBN, and catecholborane. We found that the large dihedral angle (52°) between the Si═Si double bond and the boryl group plane of **3b**, which prevents π-conjugation between the Si═Si double bond and the vacant

Received: February 3, 2011
Published: March 15, 2011

dx.doi.org/10.1021/om200106h | *Organometallics* 2011, 30, 2044–2050

Scheme 1. Reaction of Disilyne 1 with Hydroboranes, Giving Hydroboration Products 3

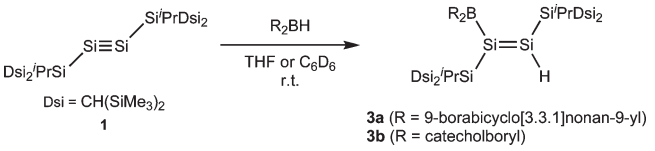

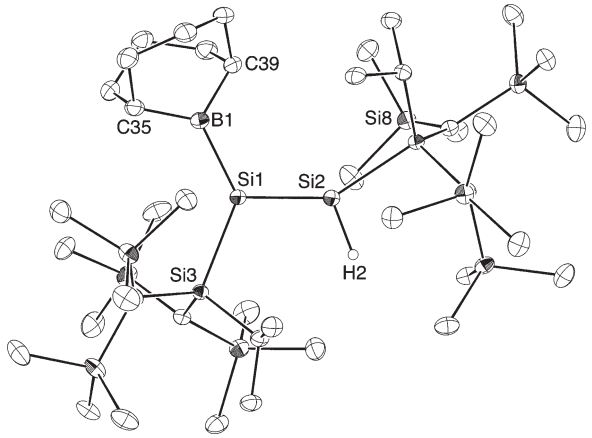

Figure 1. ORTEP drawing of **3a** (30% thermal ellipsoids). Hydrogen atoms except for H2 on Si2 and the toluene molecule as a crystallization solvent are omitted for clarity.

2p-orbital on the boron atom, is in contrast to the nearly coplanar arrangement of **3a**. We also discuss the correlation between the contribution of π-conjugation and the dihedral angle between the Si=Si double bond and the boryl group plane, using theoretical studies. Furthermore, we report theoretical studies on the mechanism of this reaction, showing that these reactions involve an interaction between the HOMO (π_{out}) of the disilyne and the LUMO (vacant 2p-orbital) of the borane in the initial step, followed by several consecutive steps to form the boryl-substituted disilene.

RESULTS AND DISCUSSION

1. Synthesis, Structure, and Properties of Boryl-Substituted Disilenes. In an earlier study, we described the reaction of disilyne **1** with 9-BBN in THF to produce the corresponding boryl-substituted disilene R(R′$_2$B)Si=SiHR **3a** (R′$_2$B = 9-bora-[3.3.1]nonan-9-yl) (Scheme 1).[24a] The reaction of disilyne **1** with catecholborane in C_6D_6 at room temperature also afforded boryl-substituted disilene R(R′$_2$B)Si=SiHR **3b** (R′$_2$B = catecholboryl), which was isolated as air- and moisture-sensitive yellow crystals in 28% yield (Scheme 1). Despite the fact that 9-BBN is bulkier than catecholborane, the reaction with 9-BBN to form **3a** was faster than that with catecholborane to form **3b** (4 and 50 h for completion, respectively), because of the decreased electrophilicity of the catecholborane due to the presence of oxygen atoms.

The solid-state structures of **3a** and **3b** were determined by X-ray crystallography and are shown in Figures 1 and 2. Selected bond lengths and bond angles are listed in Table 1. In both **3a** and **3b**, the sums of the bond angles around the boron atom and skeletal Si atoms are nearly 360°; however, the orientation of the boryl substituent plane to the Si=Si double bond exhibits a marked contrast. **3a** has almost planar geometry with the torsion angle of

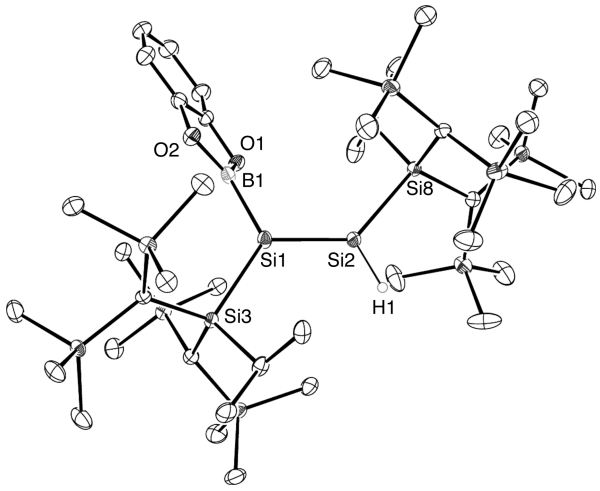

Figure 2. ORTEP drawing of **3b** (50% thermal ellipsoids). Hydrogen atoms are omitted for clarity.

Table 1. Selected Bond Lengths and Angles of 3a and 3b

	3a	3b
	Bond Lengths (Å)	
Si1−Si2	2.1838(12)	2.1634(12)
Si1−Si3	2.3872(11)	2.3875(13)
Si1−B1	2.002(4)	1.996(4)
Si2−Si8	2.3733(11)	2.3647(13)
Si2−H2	1.42(3)	1.41(3)
B1−E1	1.573(5) (B1−C35)	1.389(4) (B1−O1)
B1−E2	1.577(5) (B1−C39)	1.397(4) (B1−O2)
	Bond Angles (deg)	
Si2−Si1−Si3	111.08(4)	124.40(5)
Si2−Si1−B1	116.89(11)	112.29(12)
Si3−Si1−B1	131.94(11)	121.36(11)
Si1−Si2−Si8	145.86(5)	131.71(5)
Si1−Si2−H2	111.2(13)	114.4(14)
Si8−Si2−H2	102.6(13)	112.6(14)
ΣB1	126.9(2) (Si1−B1−C35)	123.3(3) (Si1−B1−O1)
	121.7(2) (Si1−B1−C39)	126.5(3) (Si1−B1−O2)
	111.1(3) (C35−B1−C39)	110.2(3) (O1−B1−O2)

Si2−Si1−B1−C35 being ca. 18°, which allows for π-conjugation between the Si=Si bond and the boryl group. Meanwhile, **3b** has a markedly twisted arrangement, with the Si2−Si1−B1−O1 torsion angle of 52°, preventing π-conjugation. The large torsion angles in **3b** can be explained by two contributing factors: (i) twisting more effectively reduces the steric effects of the planar catecholboryl group compared with the isotropic 9-BBN group, (ii) the n-donation from oxygen atoms to the boron atom weakens the π-conjugation. The Si1−Si2 bond length of **3a** (2.1838(12) Å) is longer than that of **3b** (2.1634(12) Å), caused by the steric factor.

3a and **3b** were fully characterized by spectroscopic data as well as X-ray crystallography. In the ^{29}Si NMR spectrum of **3a**, the signals of low-coordinate silicon atoms are observed at 150.5 ppm (H−*Si*=Si) and 121.7 (B−*Si*=Si). The ^{29}Si NMR spectrum of **3b** also shows characteristic signals of skeletal silicon atoms at 123.4 (H−*Si*=Si) and 84.3 ppm (B−*Si*=Si), both of

dx.doi.org/10.1021/om200106h |*Organometallics* 2011, 30, 2044–2050

Chart 1. Resonance Structures of Boryl-Substituted Disilenes 3

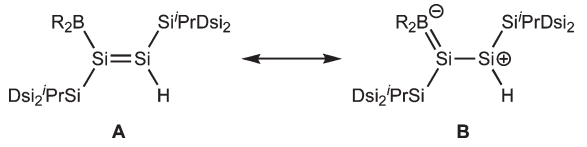

Scheme 2. Reaction of the Boryl-Substituted Disilene 3a with Methanol

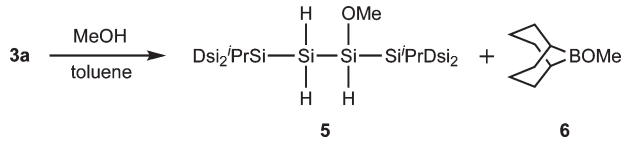

Scheme 3. Proposed Mechanism for the Reaction of the Boryl-Substituted Disilene 3a with Methanol

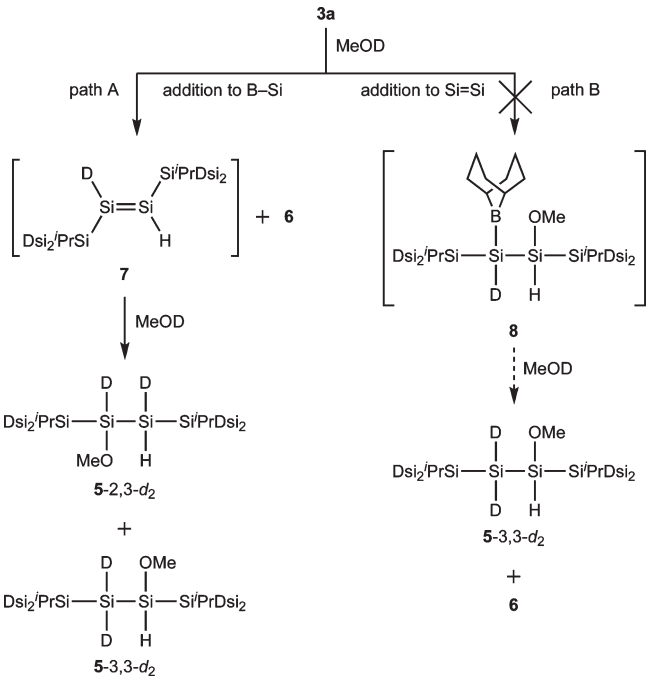

which are in accordance with the typical range for unsymmetrical disilenes.[26,27] However, the former signal shifts upfield compared with that of **3a** (150.5 ppm). In the ^{1}H NMR spectrum of **3b**, the Si—H signal (5.94 ppm) is also observed further upfield than that of **3a** (6.21 ppm). This low-field shift of the Si—H unit of **3a** compared with that of **3b** indicates a contribution from zwitterionic structure **B**, which has cationic character of the H-substituted Si atom (Chart 1). In the UV—vis spectra of **3a** and **3b**, the longest absorption maxima (λ_{max}), corresponding to $\pi-\pi^*$ electronic transitions, were observed at 469 and 411 nm, respectively. The 58 nm red shift also suggests that **3a** has stronger π-conjugation than **3b**.

The boryl-substituted disilenes **3** have two reactive sites: the Si═Si π-bond and the boron atom with a vacant p-orbital. It is quite interesting to examine the reaction of **3** with alcohol. The boryl-substituted disilene **3a** reacted with MeOH from −78 °C to room temperature to give methoxydisilane **5** and methoxyborane **6** quantitatively (Scheme 2), accompanied by cleavage of the B—Si bond in **3a**. To clarify the mechanism of this reaction, MeOD was reacted with **3a** in the same manner. As a result, a nearly 1:1 mixture of **5**-2,3-d_2 and **5**-3,3-d_2 was produced along with **6**, implying that the initial step is B—Si bond cleavage, which affords dihydrodisilene **7** as an intermediate (Scheme 3, path A). The alternative route (path B), which proceeds by initial attack of MeOH(D) at the β-Si atom of the boryl-substituted disilene, reflecting the polarity of the Si═Si double bond, to give 1-boryl-2-methoxydisilane **8**, can be ruled out because of the presence of **5**-2,3-d_2.

2. Theoretical Studies. Although the NMR and UV—vis spectra of boryl-substituted disilenes **3a** and **3b** explicitly show the correlation between π-conjugation and the dihedral angle between the Si═Si double-bond plane and the boryl group plane, the Si═Si double-bond and Si—B single-bond lengths of **3a** and **3b** do not conform to the resonance structure in Chart 1. Thus, we calculated the optimized model compound $Me_3Si(Me_2B)Si{=}Si(H)SiMe_3$ (**3′**), fixing the dihedral angle θ between the boryl group plane and the Si═Si double-bond plane every 15° from 0° to 90° (Figure 3). These calculations were performed at the B3LYP/6-31G(d)[28,29] level of theory using the Gaussian 03 package.[30]

The potential energy curve in Figure 3a shows that the nearly planar model with θ = 15° was a local minimum. As the dihedral angle θ increases above 15°, the relative energies of the model disilenes increase in incremental steps due to the decrease in the π-overlap between the vacant 2p-orbital of the boron atom and the π-orbital of the Si═Si double bond (Figure 3a). However, the most destabilized θ = 90° model is only 3.2 kcal/mol less stable than the local minimum. As shown in Figure 3b and c, as the dihedral angle θ increases above 15°, the Si—B bond length increases and the Si═Si double bond length decreases. Thus, the Si—B single-bond and the Si═Si double-bond lengths of the model disilene reflect the contribution of zwitterionic structure **B** (Chart 1).

GIAO calculations of the optimized model disilene **3′** using the B3LYP/6-311G(3d)[29] basis set are also consistent with the contribution of zwitterionic structure **B** in Chart 1 (Figure 3d). Although the calculated $\delta(^{29}Si)$ chemical shifts of the B-substituted low-coordinated silicon atom do not change much with the increase in the dihedral angle θ, from 151.3 (θ = 0°) to 161.2 ppm (θ = 90°), the $\delta(^{29}Si)$ values of the H-substituted low-coordinated silicon atom are shifted significantly upfield, from 189.2 (θ = 0°) to 105.4 ppm (θ = 90°). These results clearly show the increase in the cationic character on the H-substituted low-coordinated silicon atom, which is indicated by the zwitterionic structure **B** (Chart 1), as the Si═Si double-bond plane and boryl group plane become coplanar. The calculated NPA charges of the H-substituted low-coordinated silicon atom also show a decrease in the cationic charge as the dihedral angle θ increases (NPA charge: +0.119 for θ = 0° and +0.013 for θ = 90°).

To understand the reaction mechanism, we performed calculations for the 1,2-addition of BH_3 to disilyne using a $SiMe_3$ group instead of $Si^iPr[CH(SiMe_3)_2]_2$. The reaction path was calculated at the B3LYP level using the 6-31+G(d) basis set. Figure 4 depicts the energy profile of the reaction of the simplified disilyne with borane and optimized geometries of the intermediates **Int1** and the products **Pro1** and **Pro2** (*Z*- and *E*-boryl-substituted disilenes) together with the transition state **TS1**, which connects **Int1** and **Pro1**. The transition state **TS1** is found as a nearly four-center-like structure with a clearly

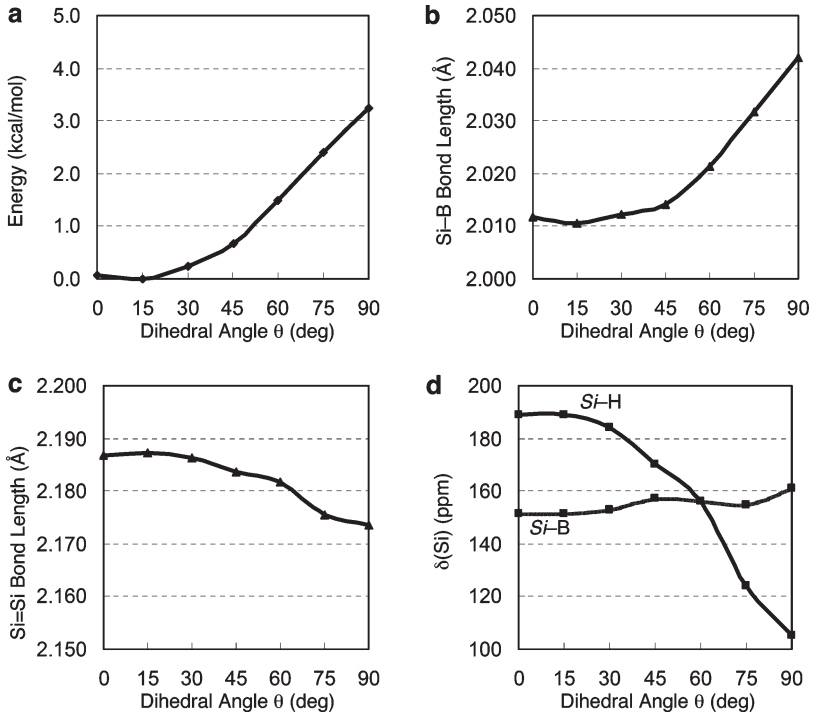

Figure 3. Theoretical calculations on $H_3Si(Me_2B)Si{=}Si(H)SiH_3$ (**3′**) as a function of the dihedral angle between the Si=Si and the boryl group planes at the GIAO//B3LYP/6-311G(3d)//B3LYP/6-31G(d) level: (a) relative energies, (b) Si−B bond lengths, (c) Si=Si double-bond lengths, and (d) chemical shifts of skeletal silicon atoms.

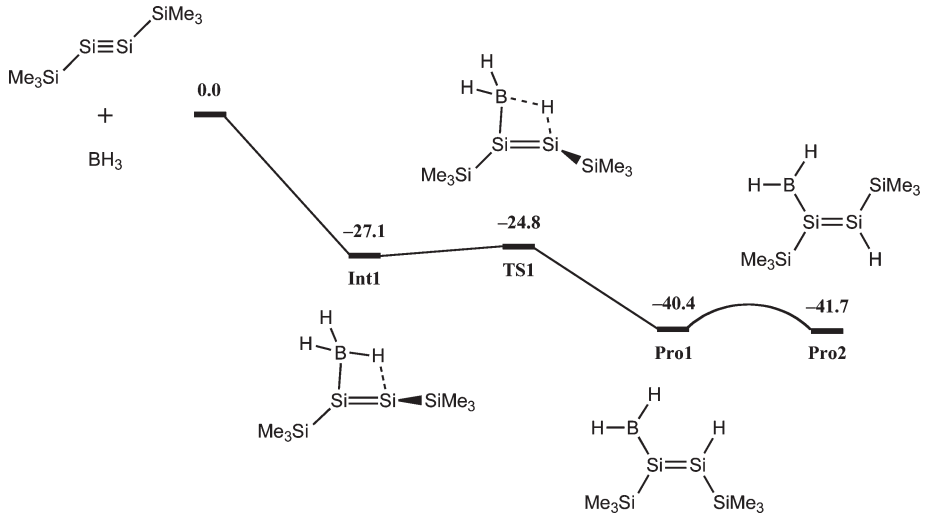

Figure 4. Potential energy profile for reaction of disilyne **3′** ($Me_3SiSi{\equiv}SiSiMe_3$) with BH_3 (energy in kcal/mol) calculated at the B3LYP/6-31+G(d) level.

elongated B−H bond (1.820 Å). The optimized structures of **Int1** and **TS1** are similar to those reported for the reaction of disilenes with BH_3.[31] On the other hand, neither a transition state between **Pro1** and **Pro2** nor a pathway leading directly to **Pro2** was found. Nevertheless, in general, the activation free energies for *E*,*Z*-isomerization of silyl-substituted disilenes are sufficiently low to allow facile rotation around the Si=Si bonds even at room temperature.[27] In addition, the bulky $Si^iPr[CH(SiMe_3)_2]_2$ groups of **3a** and **3b** would accelerate *E*,*Z*-isomerization to reduce steric hindrance. **Int1** has an elongated Si−H bond (1.716 Å) compared with **Pro1** (1.496 Å) and a large negative value for the total natural charge of the BH_3 unit (−0.64). These results suggest that the first step in the reaction is an interaction between the out-of-plane HOMO (π_{out}) of the disilyne and the LUMO (vacant 2p-orbital) of the borane, resulting in σ-coordination to produce **Int1**.

■ CONCLUSION

In summary, the synthesis and full characterization of boryl-substituted disilenes **3a** and **3b** were accomplished by the reaction of disilyne **1** with 9-BBN and catecholborane. The

dx.doi.org/10.1021/om200106h |*Organometallics* 2011, 30, 2044–2050

spectroscopic and structural data of **3a** and **3b** and theoretical studies of the model compound of boryl-substituted disilenes **3′** clearly demonstrate that the dihedral angle between the Si═Si double-bond plane and the boryl group plane has a large influence on the π-conjugation between the π-orbital of the disilene and the vacant 2p-orbital on the boron atom. Theoretical calculations on the reaction between the disilyne and borane show that the reaction proceeds via interaction of the HOMO (π_{out}) of the disilyne and the LUMO (vacant 2p-orbital) of the borane.

EXPERIMENTAL SECTION

General Procedures. All experiments were performed using high-vacuum line techniques or in an argon atmosphere using an MBraun MB 150B-G glovebox. All solvents were dried and degassed over potassium mirror under vacuum prior to use. NMR spectra were recorded on Bruker AC-300FT NMR (^{1}H NMR at 300.1 MHz; ^{13}C NMR at 75.5 MHz; ^{29}Si NMR at 59.6 MHz) and AV-400FT NMR (^{1}H NMR at 400 MHz; ^{13}C NMR at 100.6 MHz; ^{29}Si NMR at 79.5 MHz) spectrometers. High-resolution mass spectra were measured on a Bruker Daltonics micrOTOF-TU mass spectrometer with APCI (atmospheric pressure chemical ionization method). UV−vis spectra were recorded on a Shimadzu UV-3150 UV−vis spectrophotometer in hexane. 1,1,4,4-Tetrakis[bis(trimethylsilyl)methyl]-1,4-diisopropyltetrasila-2-yne (**1**) was prepared according to the published procedure.[10a]

Experimental Procedure and Spectral Data for 1,1,4,4-Tetrakis[bis(trimethylsilyl)methyl]-1,4-diisopropyl-2-(9-borabicyclo-[3.3.1]nonan-9-yl)]tetrasila-2-ene, 3a. Dry, oxygen-free THF (2.0 mL) was added by vacuum transfer to a mixture of 1,1,4,4-tetrakis-[bis(trimethylsilyl)methyl]-1,4-diisopropyltetrasila-2-yne (**1**) (100 mg, 0.12 mmol) and 9-borabicyclo[3.3.1]nonane (17 mg, 0.14 mmol), and the mixture was stirred at room temperature for 4 h. The color of the solution changed to orange from the emerald green of **1**. After evaporation, the residue was recrystallized from pentane (0.5 mL) at −30 °C to give **3** as air- and moisture-sensitive orange crystals (62 mg, 53% yield): mp 129.9−130.8 °C (dec); ^{1}H NMR (C_7D_8, δ) 0.19 (s, 2 H, C*H*(SiMe$_3$)$_2$), 0.20 (s, 2 H, C*H*(SiMe$_3$)$_2$), 0.32 (s, 18 H, CH(Si*Me*$_3$)$_2$), 0.40 (s, 18 H, CH(Si*Me*$_3$)$_2$), 0.417 (s, 18 H, CH(Si*Me*$_3$)$_2$), 0.423 (s, 18 H, CH(Si*Me*$_3$)$_2$), 1.35 (d, J = 7.5 Hz, 6 H, CH(C*H*$_3$)$_2$), 1.42 (d, J = 7.5 Hz, 6 H, CH(C*H*$_3$)$_2$), 1.60 (sept, J = 7.5 Hz, 1 H, C*H*(CH$_3$)$_2$), 1.94 (sept, J = 7.5 Hz, 1 H, C*H*(CH$_3$)$_2$), 1.90−2.06 (m, 8 H, CH$_2$C*H*$_2$CH), 2.13−2.19 (m, 4 H, CH$_2$C*H*$_2$CH$_2$), 2.67 (br, 2 H, C*H*−B), 6.21 (s, 1 H, Si*H*); ^{13}C NMR (C_7D_8, δ) 5.1 (Si*Me*$_3$ × 2), 5.4 (Si*Me*$_3$), 6.5 (Si*Me*$_3$), 8.6 (CH(SiMe$_3$)$_2$ × 2), 17.4 (*C*H(CH$_3$)$_2$), 17.5 (*C*H(CH$_3$)$_2$), 20.8 (br, CH(*C*H$_3$)$_2$), 21.7 (CH(*C*H$_3$)$_2$), 23.0 (*C*H$_2$), 34.3 (*C*H$_2$), 35.7 (*C*H−B); ^{29}Si NMR (C_7D_8, δ) −0.7 (*Si*Me$_3$), −0.5 (*Si*Me$_3$), 0.0 (*Si*Me$_3$ × 2), 7.3 (*Si*^{i}PrDsi$_2$), 14.6 (*Si*^{i}PrDsi$_2$), 121.7 (Si═*Si*−B), 150.5 (d, $^1J_{Si-H}$ = 157 Hz, Si═*Si*−H); HRMS (APCI) m/z calcd for $C_{42}H_{105}BSi_{12}$ M^+ 956.5563, found 956.5545; UV/vis (hexane) λ_{max}/nm (ε) 307 (1280), 469 (3050).

Experimental Procedure and Spectral Data for 1,1,4,4-Tetrakis-[bis(trimethylsilyl)methyl]-2-catecholboryl-1,4-diisopropyltetrasila-2-ene, 3b. Dry, oxygen-free catecholborane (20 μL, 0.19 mmol) was added by microsyringe to a dry, oxygen-free C_6D_6 solution (0.5 mL) of **1** (100 mg, 0.12 mmol) in an NMR tube, and the reaction mixture was monitored by ^{1}H NMR. After 50 h, the disilyne **1** was consumed and the color of the solution changed to yellow. After evaporation, the residue was recrystallized from pentane (0.2 mL) at −30 °C to give **3b** as air- and moisture-sensitive yellow crystals (32 mg, 28% yield): mp 107.2−108.6 °C; ^{1}H NMR (C_6D_6, δ) 0.15 (s, 2 H, C*H*(SiMe$_3$)$_2$), 0.25 (s, 2 H, C*H*(SiMe$_3$)$_2$), 0.32 (s, 18 H, CH(Si*Me*$_3$)$_2$), 0.39 (s, 18 H, CH(Si*Me*$_3$)$_2$), 0.43 (s, 18 H, CH(Si*Me*$_3$)$_2$), 0.44 (s, 18 H, CH(Si*Me*$_3$)$_2$), 1.28 (d, J = 7.2 Hz, 6 H, CH(C*H*$_3$)$_2$), 1.43 (d, J = 7.2 Hz, 6 H, CH(C*H*$_3$)$_2$), 1.66−1.78 (m, 2 H, C*H*(CH$_3$)$_2$ × 2), 5.94 (s, 1 H, Si*H*), 6.82 (dd, J = 3.4, 7.8 Hz, 2 H, cat), 7.17 (dd, J = 3.4, 7.8 Hz, 2 H, cat); ^{13}C NMR (C_6D_6, δ) 5.2 (Si*Me*$_3$), 5.6 (Si*Me*$_3$), 5.7 (Si*Me*$_3$), 5.8 (Si*Me*$_3$), 6.7 (CH(SiMe$_3$)$_2$), 7.6 (CH(SiMe$_3$)$_2$), 17.2 (CH(*C*H$_3$)$_2$), 17.7 (CH(*C*H$_3$)$_2$), 21.7 (CH(*C*H$_3$)$_2$), 21.8 (CH(*C*H$_3$)$_2$), 112.6 (cat-CH), 123.2 (cat-CH), 148.8 (cat-CO); ^{29}Si NMR (C_6D_6, δ) −0.22 (*Si*Me$_3$), −0.19 (*Si*Me$_3$), 0.0 (*Si*Me$_3$), 0.2 (*Si*Me$_3$), 9.9 (*Si*^{i}PrDsi$_2$), 11.3 (*Si*^{i}PrDsi$_2$), 84.3 (═*Si*−B), 123.4 (d, $^1J_{Si-H}$ = 174 Hz, ═*Si*−H); HRMS m/z calcd for $C_{40}H_{94}{}^{11}BO_2Si_{12}$ $[M - H]^+$ 953.4573, found 953.4569; UV/vis (hexane) λ_{max}/nm (ε): 278 (12 850), 411 (8740).

Table 2. Crystallographic Data and Experimental Parameters for the Structure Analysis of 3a and 3b

	3a	3b
empirical formula	$C_{49}H_{113}BSi_{12}$	$C_{40}H_{95}BO_2Si_{12}$
formula mass (g mol^{-1})	1050.28	956.05
cryst size/mm	0.40 × 0.10 × 0.05	0.21 × 0.10 × 0.05
cryst color	orange	yellow
collection temp (K)	150	120
λ(Mo Kα) (Å)	0.71070	0.71073
cryst syst	monoclinic	triclinic
space group	P 2$_1$/c	P −1
unit cell params		
a (Å)	15.4210(5)	10.4283(6)
b (Å)	11.5920(4)	15.1729(9)
c (Å)	37.1120(7)	19.7512(11)
α (deg)	90	101.0390(10)
β (deg)	98.946(2)	90.5270(10)
γ (deg)	90	108.3180(10)
V (Å^3)	6553.4(3)	2903.8(3)
Z	4	2
D_{calc} (g cm^{-3})	1.065	1.093
F(000)	2320	1048
μ (mm^{-1})	0.266	0.297
collected reflns	56 033	31 308
indep reflns	11 031	12 707
R_{int}	0.0610	0.0497
reflns used ($I > 2.00\sigma(I)$)	11031	12707
parameters	564	500
$R_1{}^a$ [$I > 2\sigma(I)$]	0.0506	0.0522
$wR_2{}^b$ (all data)	0.1365	0.1114
S^c	1.051	1.079

^{a} $R_1 = \Sigma||F_o| - |F_c||/\Sigma|F_o|$. ^{b} $wR_2 = \{\Sigma[w(F_o{}^2 - F_c{}^2)^2]/\Sigma[w(F_o{}^2)^2]\}^{0.5}$. ^{c} $S = \{\Sigma[w(F_o{}^2 - F_c{}^2)^2]/(n-p)\}^{0.5}$, where n is the number of reflections and p is the number of parameters.

X-ray Crystallography. The single crystals of **3a** and **3b** for X-ray diffraction analysis were grown from a toluene solution (for **3a**) and a pentane solution (for **3a**). Diffraction data were collected at 150 K on a Mac Science DIP2030 image plate diffractometer with a rotating anode (50 kV, 90 mA) employing graphite-monochromatized Mo Kα radiation (λ = 0.71070 Å) for **3a** and at 120 K on a Bruker APEXII CCD area detector with a rotating anode (50 kV, 24 mA) employing graphite-monochromatized Mo Kα radiation (λ = 0.71073 Å) for **3b**. The structures were solved by the direct method, using the SHELXS-97 program, and refined by using the SHELXL-97 program.[32] The crystal data and experimental parameters for the X- ray analysis of **3a** and **3b** are listed in Tables 1 and 2. For the crystal data of **3a**, see the Supporting Information in ref 24.

Reaction of the Boryl-Substituted Disilene 3a with MeOH. Dry, oxygen-free methanol (0.10 mL, 79 mg, 2.5 mmol) was added by vacuum transfer to a dry, oxygen-free toluene solution (1.0 mL) of **3a** (32 mg, 0.033 mmol), and the mixture was stirred from −78 °C to room

temperature over 2 h. The orange color of the solution gradually disappeared. After evaporation of the solvent and remaining methanol, the ^{1}H NMR spectrum showed the presence of **5** and 9-methoxy-9-borabicyclo-[3.3.1]nonane (**6**). The residue was recrystallized from pentane (0.5 mL) at room temperature to give **5** as a colorless powder (20 mg, 69% yield): mp 142.3−144.2 °C; ^{1}H NMR (C_6D_6, δ) 0.05 (s, 2 H, C*H*($SiMe_3$)$_2$), 0.16 (s, 1 H, C*H*($SiMe_3$)$_2$), 0.20 (s, 1 H, C*H*($SiMe_3$)$_2$), 0.32 (s, 18 H, CH($SiMe_3$)$_2$), 0.345 (s, 9 H, CH($SiMe_3$)$_2$), 0.350 (s, 18 H, CH($SiMe_3$)$_2$), 0.38 (s, 9 H, CH($SiMe_3$)$_2$), 0.40 (s, 9 H, CH($SiMe_3$)$_2$), 0.43 (s, 9 H, CH($SiMe_3$)$_2$), 1.29 (d, J = 7.2 Hz, 3 H, CH(C*H*$_3$)$_2$), 1.31 (d, J = 7.2 Hz, 3 H, CH(C*H*$_3$)$_2$), 1.36 (d, J = 7.2 Hz, 3 H, CH(C*H*$_3$)$_2$), 1.41 (d, J = 7.2 Hz, 3 H, CH(C*H*$_3$)$_2$), 1.50 (sept, J = 7.2 Hz, 1 H, C*H*(CH$_3$)$_2$), 1.58 (sept, J = 7.2 Hz, 1 H, C*H*(CH$_3$)$_2$), 3.45 (d, J = 5.6 Hz, 1 H, Si*H*$_2$), 3.50 (s, 3 H, O*Me*), 3.66 (dd, J = 5.6, 9.6 Hz, 1 H, Si*H*$_2$), 5.89 (d, J = 9.6 Hz, 1 H, Si*H*(OMe)); ^{13}C NMR (C_6D_6, δ) 5.16 (Si*Me*$_3$), 5.18 (Si*Me*$_3$ × 2), 5.23 (Si*Me*$_3$), 5.32 (Si*Me*$_3$), 5.36 (Si*Me*$_3$), 5.41 (Si*Me*$_3$), 5.52 (Si*Me*$_3$), 5.6 (*C*H(SiMe$_3$)$_2$), 6.1 (*C*H(SiMe$_3$)$_2$), 7.8 (*C*H-(SiMe$_3$)$_2$), 7.9 (*C*H(SiMe$_3$)$_2$), 17.7 (CH(CH$_3$)$_2$), 17.8 (CH(CH$_3$)$_2$), 21.2 (CH(CH$_3$)$_2$), 21.7 (CH(CH$_3$)$_2$), 21.8 (CH(CH$_3$)$_2$), 21.9 (CH(CH$_3$)$_2$), 57.0 (O*Me*); ^{29}Si NMR (C_6D_6, δ) −96.7 ($^1J_{Si-H}$ = 167 Hz, *Si*H$_2$), −0.4 (*Si*Me$_3$), −0.2 (*Si*Me$_3$), −0.14 (*Si*Me$_3$), −0.09 (*Si*Me$_3$), 0.1 (*Si*Me$_3$), 0.2 (*Si*Me$_3$), 0.4 (*Si*Me$_3$), 0.6 (*Si*Me$_3$), 4.3 (*Si*^{i}PrDsi$_2$), 8.3 ($^1J_{Si-H}$ = 173 Hz, *Si*H(OMe)), 10.6 (*Si*^{i}PrDsi$_2$); HRMS m/z calcd for $C_{35}H_{95}OSi_{12}$ [M − H]$^+$ 867.4609, found 867.4610.

Reaction of the Boryl-Substituted Disilene 3a with MeOD. The procedure was the same as for the preparation of **5**, except that methanol-d_1 (0.10 mL, 79 mg, 2.5 mmol) was used to provide colorless **5**-d_2 (15 mg, 53%). ^{1}H NMR analysis showed that **5**-d_2 is a mixture of 50% **5**-2,3-d_2 and 50% **5**-3,3-d_2.

Computational Method. All calculations were carried out using the Gaussian 03 program.[29] Calculations were performed with hybrid density functional theory at the B3LYP[27,28] level, using the basis set 6-31G(d)[29] for geometry optimization, 6-311G(3d)[28] for the GIAO method, and 6-31+G(d)[29] for the transition state searches.

■ ASSOCIATED CONTENT

Supporting Information. Tables of crystallographic data including atomic positional and thermal parameters for **3b** (PDF/CIF) and computational details (tables of atomic coordinates for optimized geometries of the model compound **3′** and values of their total energies). This material is available free of charge via the Internet at http://pubs.acs.org.

■ AUTHOR INFORMATION

Corresponding Author

*Phone: +81-29-853-4314. Fax: +81-29-853-4314 E-mail: sekiguch@chem.tsukuba.ac.jp.

■ ACKNOWLEDGMENT

This work was financially supported by Grants-in-Aid for Scientific Research program (Nos. 19105001, 20038006, 21550033) from the Ministry of Education, Science, Sports, and Culture of Japan, JSPS Research Fellowship for Young Scientist (K.T.).

■ REFERENCES

(1) Davidson, P. J.; Lappert, M. F. *J. Chem. Soc., Chem. Commun.* **1973**, 317.

(2) West, R.; Fink, M. J.; Michl, J. *Science* **1981**, *214*, 1343.

(3) Brook, A. G.; Abdesaken, F.; Gutekunst, B.; Gutekunst, G.; Kallury, R. K. *J. Chem. Soc., Chem. Commun.* **1981**, 191.

(4) Reviews on double-bond chemistry of heavier group 14 elements:(a) Okazaki, R.; West, R. *Adv. Organomet. Chem.* **1996**, *39*, 231. (b) Weidenbruch, M. *Eur. J. Inorg. Chem.* **1999**, 373. (c) Escudié, J.; Ranaivonjatovo, H. *Adv. Organomet. Chem.* **1999**, *44*, 113.(d) Weidenbruch, M. In *The Chemistry of Organic Silicon Compounds*; Rappoport, Z.; Apeloig, Y., Eds.; Wiley: Chichester, U.K., Vol. 3, Chapter 5, 2001. (e) Klinkhammer, K. In *The Chemistry of Organic Germanium, Tin and Lead Compounds*; Rappoport, Z., Ed.; Wiley: Chichester, U.K., Vol. 2, Part 1, Chapter 4, 2002. (f) Tokitoh, N.; Okazaki, R. In *The Chemistry of Organic Germanium, Tin and Lead Compounds*; Rappoport, Z., Ed.; Wiley: Chichester, U.K., Vol. 2, Part 1, Chapter 13, 2002. (g) Weidenbruch, M. *Organometallics* **2003**, *22*, 4348. (h) Lee, V. Ya.; Sekiguchi, A. *Organometallics* **2004**, *23*, 2822. (i) Kira, M.; Iwamoto, T. *Adv. Organomet. Chem.* **2006**, *54*, 73. (j) Lee, V. Ya.; Sekiguchi, A.; Escudié, J.; Ranaivonjatovo, H. *Chem. Lett.* **2010**, *39*, 312.

(5) Recent reviews on the triple-bond chemistry of heavier group 14 elements: (a) Power, P. P. *Chem. Rev.* **1999**, *99*, 3463. (b) Weidenbruch, M. *J. Organomet. Chem.* **2002**, *646*, 39. (c) Power, P. P. *Chem. Commun.* **2003**, 2091. (d) Weidenbruch, M. *Angew. Chem., Int. Ed.* **2004**, *43*, 2. (e) Power, P. P. *Appl. Organomet. Chem.* **2005**, *19*, 488. (f) Sekiguchi, A.; Ichinohe, M.; Kinjo, R. *Bull. Chem. Soc. Jpn.* **2006**, *79*, 825. (g) Power, P. P. *Organometallics* **2007**, *26*, 4362. (h) Sekiguchi, A. *Pure Appl. Chem.* **2008**, *80*, 447. (i) Power, P. P. *Nature* **2010**, *463*, 171. (j) Sasamori, T.; Han, J.-S.; Hironaka, K.; Takagi, N.; Nagase, N.; Tokitoh, N. *Pure Appl. Chem.* **2010**, *82*, 603.

(6) Pu, L.; Twamley, B.; Power, P. P. *J. Am. Chem. Soc.* **2000**, *122*, 3524.

(7) (a) Stender, M.; Phillips, A. D.; Wright, R. J.; Power, P. P. *Angew. Chem., Int. Ed.* **2002**, *41*, 1785. (b) Fischer, R. C.; Pu, L.; Fettinger, J. C.; Brynda, M. A.; Power, P. P. *J. Am. Chem. Soc.* **2006**, *128*, 11366.

(8) Phillips, A. D.; Wright, R. J.; Olmstead, M. M.; Power, P. P. *J. Am. Chem. Soc.* **2002**, *124*, 5930.

(9) Sugiyama, Y.; Sasamori, T.; Hosoi, Y.; Furukawa, Y.; Takagi, N.; Nagase, S.; Tokitoh, N. *J. Am. Chem. Soc.* **2006**, *128*, 1023.

(10) (a) Sekiguchi, A.; Kinjo, R.; Ichinohe, M. *Science* **2004**, *305*, 1755. Also see:(b) Kravchenko, V.; Kinjo, R.; Sekiguchi, A.; Ichinohe, M.; West, R.; Balazs, Y. S.; Schmidt, A.; Karni, M.; Apeloig, Y. *J. Am. Chem. Soc.* **2006**, *128*, 14472.

(11) Wiberg, N.; Vasisht, S. K.; Fischer, G.; Mayer, P. *Z. Anorg. Allg. Chem.* **2004**, *630*, 1823.

(12) Sasamori, T.; Hironaka, K.; Sugiyama, Y.; Takagi, N.; Nagase, S.; Hosoi, Y.; Furukawa, Y.; Tokitoh, N. *J. Am. Chem. Soc.* **2008**, *130*, 13856.

(13) Murata, Y.; Ichinohe, M.; Sekiguchi, A. *J. Am. Chem. Soc.* **2010**, *132*, 16768.

(14) Kinjo, R.; Ichinohe, M.; Sekiguchi, A.; Takagi, N.; Sumimoto, M.; Nagase, S. *J. Am. Chem. Soc.* **2007**, *129*, 7766.

(15) Kinjo, R.; Ichinohe, M.; Sekiguchi, A. *J. Am. Chem. Soc.* **2007**, *129*, 26.

(16) Yamaguchi, T.; Ichinohe, M.; Sekiguchi, A. *New J. Chem.* **2010**, *34*, 1544.

(17) Sekiguchi, A.; Kinjo, R.; Ichinohe, M. *Synth. Met.* **2009**, *159*, 773.

(18) Takeuchi, K.; Ichinohe, M.; Sekiguchi, A.; Guo, J.-D.; Nagase, S. *Organometallics* **2009**, *28*, 2658.

(19) Takeuchi, K.; Ichinohe, M.; Sekiguchi, A. *J. Am. Chem. Soc.* **2008**, *130*, 16848.

(20) Takeuchi, K.; Ichinohe, M.; Sekiguchi, A.; Guo, J.-D.; Nagase, S. *J. Phys. Org. Chem.* **2010**, *23*, 390.

(21) Han, J. S.; Sasamori, T.; Mizuhata, Y.; Tokitoh, N. *J. Am. Chem. Soc.* **2010**, *132*, 2546.

(22) Han, J. S.; Sasamori, T.; Mizuhata, Y.; Tokitoh, N. *Dalton Trans.* **2010**, *39*, 9238.

(23) Yamaguchi, T.; Sekiguchi, A.; Driess, M. *J. Am. Chem. Soc.* **2010**, *132*, 14061.

(24) (a) Takeuchi, K.; Ikoshi, M.; Ichinohe, M.; Sekiguchi, A. *J. Am. Chem. Soc.* **2010**, *132*, 930. (b) Takeuchi, K.; Ichinohe, M.; Sekiguchi, A. *J. Organomet. Chem.* **2011**, *696*, 1156.

(25) Inoue, S.; Ichinohe, M.; Sekiguchi, A. *Chem. Lett.* **2008**, *37*, 1044.
(26) Ichinohe, M.; Arai, Y.; Sekiguchi, A. *Organometallics* **2001**, *20*, 4141.
(27) (a) Lee, V. Ya.; Sekiguchi, A. *Organometallic Compounds of Low-Coordinate Si, Ge, Sn, and Pb: From Phantom Species to Stable Compounds*; Wiley: Chichester, 2010; Chapter 5. (b) Scheschkewitz, D. *Chem.—Eur. J.* **2009**, *15*, 2476. (c) Scheschkewitz, D. *Chem. Lett.* **2011**, *40*, 2.
(28) (a) Becke, A. D. *J. Chem. Phys.* **1993**, *98*, 5648. (b) Stephens, P. J.; Devlin, F. J.; Chabalowski, C. F.; Frisch, M. J. *J. Phys. Chem.* **1994**, *98*, 11623.
(29) Lee, C.; Yang, W.; Parr, R. G. *Phys. Rev. B* **1988**, *37*, 785.
(30) Frisch, M. J.; Trucks, G. W.; Schlegel, H. B.; Scuseria, G. E.; Robb, M. A.; Cheeseman, J. R.; Montgomery, J. A., Jr.; Vreven, T.; Kudin, K. N.; Burant, J. C.; Millam, J. M.; Iyengar, S. S.; Tomasi, J.; Barone, V.; Mennucci, B.; Cossi, M.; Scalmani, G.; Rega, N.; Petersson, G. A.; Nakatsuji, H.; Hada, M.; Ehara, M.; Toyota, K.; Fukuda, R.; Hasegawa, J.; Ishida, M.; Nakajima, T.; Honda, Y.; Kitao, O.; Nakai, H.; Klene, M.; Li, X.; Knox, J. E.; Hratchian, H. P.; Cross, J. B.; Bakken, V.; Adamo, C.; Jaramillo, J.; Gomperts, R.; Stratmann, R. E.; Yazyev, O.; Austin, A. J.; Cammi, R.; Pomelli, C.; Ochterski, J. W.; Ayala, P. Y.; Morokuma, K.; Voth, G. A.; Salvador, P.; Dannenberg, J. J.; Zakrzewski, V. G.; Dapprich, S.; Daniels, A. D.; Strain, M. C.; Farkas, O.; Malick, D. K.; Rabuck, A. D.; Raghavachari, K.; Foresman, J. B.; Ortiz, J. V.; Cui, Q.; Baboul, A. G.; Clifford, S.; Cioslowski, J.; Stefanov, B. B.; Liu, G.; Liashenko, A.; Piskorz, P.; Komaromi, I.; Martin, R. L.; Fox, D. J.; Keith, T.; Al-Laham, M. A.; Peng, C. Y.; Nanayakkara, A.; Challacombe, M.; Gill, P. M. W.; Johnson, B.; Chen, W.; Wong, M. W.; Gonzalez, C.; Pople, J. A.*Gaussian 03*; Gaussian, Inc.: Wallingford, CT, 2004.
(31) Xu, Y.-J.; Zhang, Y.-F.; Li, J.-Q. *Chem. Phys. Lett.* **2006**, *421*, 36.
(32) Sheldrick, G. M. *Acta Crystallogr.* **2008**, *A64*, 112.